DEVELOPMENT AND MAGNETIC CHARACTERIZATION OF THAILAND'S FIRST IN-VACUUM WIGGLER PROTOTYPE

N. Wasanbongngem†, H. Nakajima, Ch. Pasatcha, S. Rugmai, R. Satasasawat, S. Soontaranon, N. Sutthimon, Synchrotron Light Research Institute, Nakhon Ratchasima, Thailand

Abstract

This paper details the development of Thailand's first prototype in-vacuum wiggler (IVW). The project began with 3D magnetic field simulations using the RADIA package to define the optimal magnetic configuration. To verify their magnetic properties and ensure field quality, individual magnet blocks are characterized using a Helmholtz coil system. The magnet arrays are assembled onto an in-vacuum girder utilizing a custom workstation and specialized keeper tools to maintain strict mechanical tolerances and ensure safety against strong magnetic forces. Optical alignment using a leveling camera verifies girder planarity and gap consistency prior to final metrology. Furthermore, this work details a custom-built Hall probe measurement bench—also driven by newly developed control and data acquisition software—which is employed for the inaugural field mapping of the assembled IVW. A preliminary comparison between the experimental field data and RADIA simulations, prior to the application of shimming or magic finger end-field corrections, is presented. This study establishes a critical technical framework for future high-performance ID development in Thailand.

INTRODUCTION

Synchrotron light sources depend on insertion devices (IDs), such as wigglers and undulators, to enhance photon flux and brightness [1]. Transitioning toward high-performance in-vacuum IDs is essential for expanding experimental capabilities. However, in-vacuum wigglers (IVWs) present significant engineering challenges, particularly regarding complex mechanical structures and precise magnetic field control within ultra-high vacuum environments [2-4].

This paper details the development of Thailand's first domestically fabricated prototype IVW. The design phase utilized 3D magnetic simulations via the RADIA package [5-8]. To manage the strong attractive forces of high-remanence magnets, specialized assembly workstations and custom keeper tools were developed to ensure both precision and safety.

To validate the simulations, a robust characterization framework was established [9]. Individual magnet blocks were characterized using a Helmholtz coil system from Kyma company with in-house developed software. Furthermore, this work describes a custom-built Hall probe measurement bench featuring a Metrolab sensor and in-house developed mechanics and control software. Initial comparisons between experimental data and RADIA simulations, conducted prior to field corrections, provide a technical framework for future ID development in Thailand.

†noppharit@slri.or.th

MAGNETIC DESIGN AND SIMULATION

Magnetic Design

The 3D magnetic geometry of the wiggler was modeled and optimized using the RADIA package integrated within the Mathematica environment. Individual permanent magnet blocks were designed with physical dimensions of 79 × 79 × 50 mm. To satisfy the stringent coercivity requirement (> 2000 kA/m). The Neodymium-Iron-Boron (NdFeB) was selected as the permanent magnet material. Correspondingly, The Vanadium Permendur was chosen for the pole structures due to its exceptionally high saturation polarization characteristics. The final magnetic configuration features 5 main poles and 2 end poles, establishing a stable magnetic period (λ_u) of 230 mm capable of providing a peak magnetic field of 2.0 T at the minimum working gap of 15 mm [5]. The detailed engineering design and clamping assembly layout of these magnet blocks and poles are illustrated in Fig. 1.

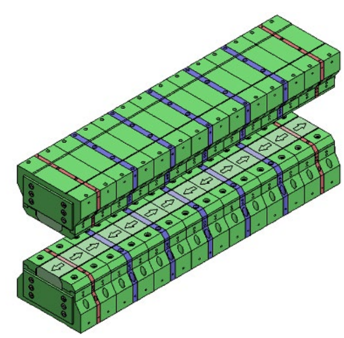

Figure 1: Mechanical design and clamping assembly layout of the wiggler magnet arrays and pole pieces.

Simulation Results and Comparative Analysis

Magnetostatic simulations were carried out across various magnetic gaps, with primary focus on 15 mm, 20 mm, and 25 mm. These simulated configurations established the theoretical baseline for the subsequent experimental magnetic characterization phases. The peak magnetic field demonstrates a clear inverse relationship with the gap size, yielding values of 2.0 T, 1.6 T, and 1.4 T at operational gaps of 15 mm, 20 mm, and 25 mm, respectively (while a maximum of 2.4 T is obtained at a tight gap of 10 mm).

The first field integral (I_1) and second field integral (I_2) profiles across the operational gaps show consistent symmetric alternating wave patterns along the beam axis.

Because the end-pole structures were explicitly optimized for the primary working gap, the simulated field integrals at this specific configuration successfully converge to zero at the device boundaries, effectively minimizing residual electron beam orbit kicks. This work focuses exclusively on the main longitudinal magnetic field component, and the field metrics for this optimized state are presented in Fig. 2.

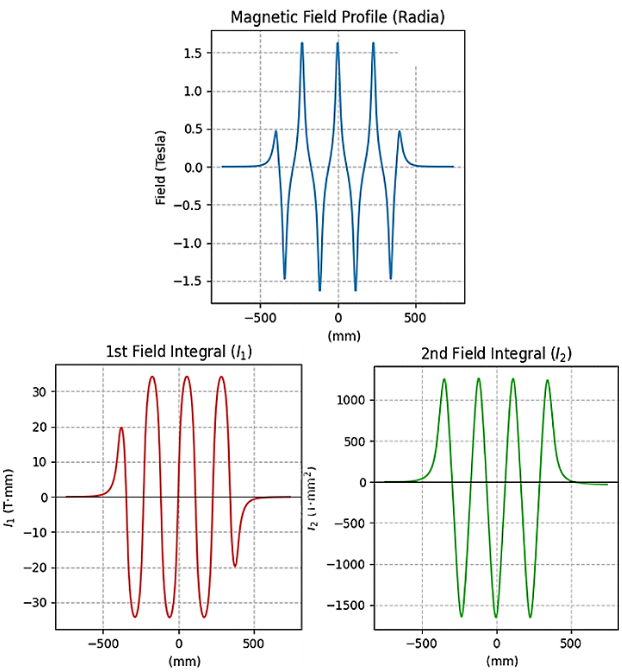

Figure 2: Simulated magnetic field profile, and field integrals (I_1, I_2) for the optimized 20 mm gap configuration.

MAGNET CHARACTERIZATION

Metrological Validation

To establish a reliable metrology baseline, the magnetic moment of a smaller magnet U60 undulator was characterized by using the Helmholtz coil. A critical cross-validation was conducted between the commercial Kyma software and a custom in-house Python analysis suite, specifically comparing the magnetization and remanence (J_r) components. The results are in excellent agreement, with the J_r value measured at 1.35 T by Kyma software and 1.33 T by the Python suite. This minor discrepancy was found to be statistically insignificant, thereby confirming the reliability of the in-house software for processing integrated voltage signals and managing the wiggler magnet database.

Repeatability and Speed Stability

The system's performance of the Helmholtz coil operated with python suite was evaluated using representative IVW magnet blocks across a speed-repeatability matrix (25 to 2000 RPM). Experimental data revealed that magnetic measurements remain highly stable and consistent at rotation speeds of 200 RPM and below. As illustrated in Fig. 3, operating within this optimal speed range ensures that experimental variables do not introduce integration errors during the large-scale characterization process.

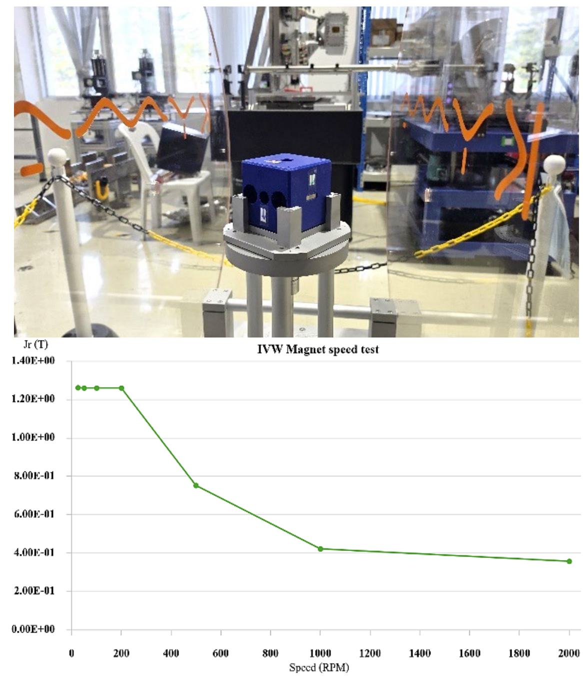

Figure 3: Measured magnetic remanence (J_r) as a function of the drive motor rotation speed in the Helmholtz coil system, demonstrating measurement stability at or below 200 RPM.

The measured J_r component were compared directly with the quality assurance certificates obtained from the magnet vendor. The results showed a high correlation, with a measured J_r of 1.26 T versus the manufacturer's value of 1.28 T. This discrepancy was considered statistically insignificant, thereby validating the laboratory's absolute accuracy and allowing for the comprehensive characterization of all remaining wiggler magnet blocks prior to final assembly.

MAGNET ASSEMBLY AND ALIGNMENT

Alignment Procedure

The mechanical alignment process began with the high-precision levelling of the workstation and the in-vacuum girders. A digital level camera and an alignment scope were utilized to ensure that the longitudinal axis of the girder was perfectly aligned with the reference coordinates of the magnet installation workstation. Furthermore, the magnet-holder modules were meticulously aligned relative to the girder surface to ensure that all structural components maintained a consistent reference plane and axial orientation prior to the introduction of the permanent magnets.

Magnet Array Installation

The installation of permanent magnets onto the in-vacuum girders was performed using a specialized assembly workstation equipped with custom fixtures and a lead screw drive system. This setup was essential for managing the significant magnetic forces encountered during the assembly of the high-remanence magnet blocks. As shown in Fig. 4, each holder-magnet assembly was carefully lifted and translated toward the girder using the lead screw mechanism to maintain strict motion control before being securely bolted into position. The final completed assembly of both the upper and lower magnet arrays is shown in Fig. 5.

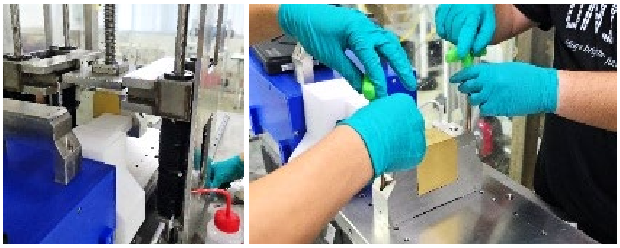

Figure 4: Mechanical integration of magnet blocks onto the girder utilizing a custom lead screw assembly system.

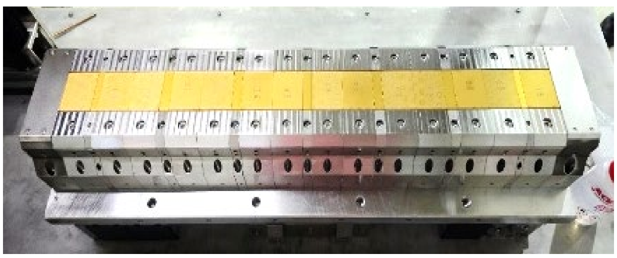

Figure 5: Final completed assembly of the upper and lower wiggler magnet arrays.

MAGNETIC MEASUREMENT RESULTS

Following the completion of the magnet array installation and mechanical alignment, experimental magnetic field measurements were conducted using a custom-built high-precision Hall probe bench. The characterization process involved scanning the magnetic field at three distinct gaps: 15, 20, and 25 mm. All measurements were performed with a constant scanning speed of 10 mm/s and a sampling rate of 5 Hz. The experimental results yielded peak magnetic fields of 1.9920 T, 1.6430 T, and 1.3790 T for the 15, 20, and 25 mm gaps, respectively. Figure 6 illustrates the magnetic field measurement setup using the Hall probe bench.

Detailed analysis of the field integral profiles indicates that the 20 mm gap configuration provides the most optimized performance. At this gap setting, the magnetic field integrals at both the entrance and exit boundaries of the device converge closest to zero compared to the other gaps. This characteristic is vital for ensuring the stability of the electron beam orbit as it traverses the insertion device. The measured magnetic field profile and the corresponding field integrals for the optimized 20 mm gap are presented in Fig. 7.

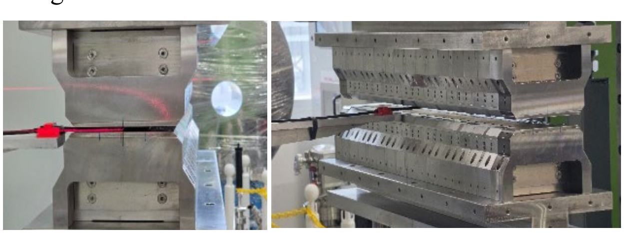

Figure 6: Magnetic field measurement setup using the custom-built Hall probe bench.

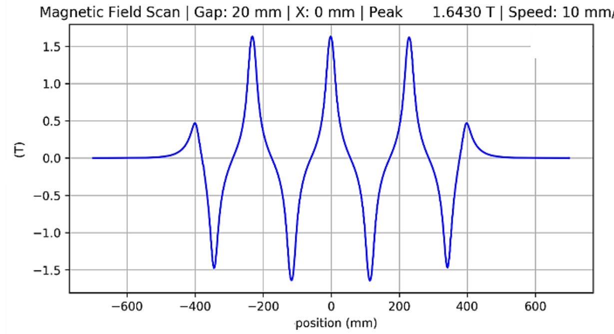

(a)

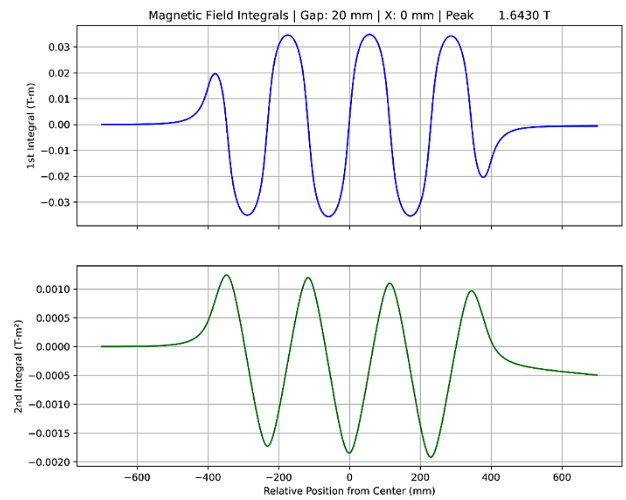

(b)

Figure 7: Experimental magnetic measurement results at the optimized 20 mm gap: (a) Measured magnetic field profile, (b) First field integral, and Second field integral.

CONCLUSION AND FUTURE ACTIVITIES

The development of Thailand's first domestically fabricated prototype in-vacuum wiggler has reached a significant milestone with the completion of its initial magnetic characterization. A comparison between the magnetostatic simulations conducted in RADIA and the experimental data obtained from the Hall probe bench demonstrates excellent agreement, particularly regarding the longitudinal magnetic field profiles and the first field integrals across the operational gaps. These results validate both the 3D magnetic design and the mechanical integrity of the wiggler's magnet array assembly.

While the primary field characteristics align well with the theoretical models, detailed analysis of the second field integral reveals a slight residual deviation from zero at the device exit, a discrepancy likely stemming from minor mechanical tolerances or material non-uniformities not captured in the idealized simulation. Consequently, future activities will focus on the calculation and implementation of magic finger end-field corrections.

This corrective shimming strategy aims to neutralize the residual field integrals and ensure the high-precision electron beam trajectory required for stable and high-performance synchrotron operation.

REFERENCES

[1] J. A. Clarke, The Science and Technology of Undulators and Wigglers. New York, NY, USA: Oxford University Press, 2004.

[2] J. C. Huang *et al.*, " Performance of a NSRRC In-Vacuum Undulator", *IEEE Trans. Appl. Supercond.*, vol. 24, no. 3, p.0503704, Jun.2014. doi:10.1109/TASC.2013.2293338

[3] T. Tanaka *et al.*, "In-Vacuum Undulators", in *Proc. FEL'05*, Palo Alto, CA, USA, Aug. 2005, paper TUOC001, pp. 370-377.

[4] Caitu Shi, Yuhui Jing, Hongliang Lu, Dashi Li and Dingchang Xian, "Design of an in-vacuum multipole wiggler for the BSRF", in *Proc. APAC'01*, Beijing, China, Sep. 2001, paper WEP028, pp. 331-333.

[5] H. Nakajima *et al.*, "Magnetic field simulation of in-vacuum permanent magnet multipole wiggler," *J. Phys.: Conf. Ser.*, vol. 3010, no. 1, p. 012007, May 2025. doi:10.1088/1742-6596/3010/1/012007

[6] O. Chubar, P. Elleaume, and J. Chavanne, "A three-dimensional magnetostatics computer code for insertion devices," *J Synchrotron Rad*, vol. 5, no. 3, pp. 481–484, May 1998. doi:10.1107/s0909049597013502

[7] P. Elleaume, O. Chubar, and J. Chavanne, "Computing 3D magnetic fields from insertion devices", in *Proc. PAC'97*, Vancouver, Canada, May 1997, pp. 3509-3511. doi:10.1109/PAC.1997.753258

[8] O. Marcouille *et al.*, "In vacuum permanent magnet wiggler optimized for the production of hard x rays," *Phys. Rev. ST Accel. Beams*, vol. 16, no. 5, May 2013. doi:10.1103/physrevstab.16.050702

[9] J. Campmany, J. Marcos, and V. Massana, "New Improvements in Magnetic Measurements Laboratory of the ALBA Synchrotron Facility," Physics Procedia, vol. 75, pp. 1214–1221, 2015. doi:10.1016/j.phpro.2015.12.123